

Hydroplasticization of latex films with varying methacrylic acid content

Citation for published version (APA):

Voogt, B., Huinink, H., van de Kamp - Peeters, L., Erich, B., Scheerder, J., Venema, P., & Adan, O. (2019). Hydroplasticization of latex films with varying methacrylic acid content. *Polymer*, 166, 206-214. Advance online publication. <https://doi.org/10.1016/j.polymer.2019.01.074>

DOI:

[10.1016/j.polymer.2019.01.074](https://doi.org/10.1016/j.polymer.2019.01.074)

Document status and date:

Published: 12/03/2019

Document Version:

Accepted manuscript including changes made at the peer-review stage

Please check the document version of this publication:

- A submitted manuscript is the version of the article upon submission and before peer-review. There can be important differences between the submitted version and the official published version of record. People interested in the research are advised to contact the author for the final version of the publication, or visit the DOI to the publisher's website.
- The final author version and the galley proof are versions of the publication after peer review.
- The final published version features the final layout of the paper including the volume, issue and page numbers.

[Link to publication](#)

General rights

Copyright and moral rights for the publications made accessible in the public portal are retained by the authors and/or other copyright owners and it is a condition of accessing publications that users recognise and abide by the legal requirements associated with these rights.

- Users may download and print one copy of any publication from the public portal for the purpose of private study or research.
- You may not further distribute the material or use it for any profit-making activity or commercial gain
- You may freely distribute the URL identifying the publication in the public portal.

If the publication is distributed under the terms of Article 25fa of the Dutch Copyright Act, indicated by the "Taverne" license above, please follow below link for the End User Agreement:

www.tue.nl/taverne

Take down policy

If you believe that this document breaches copyright please contact us at:

openaccess@tue.nl

providing details and we will investigate your claim.

Hydroplasticization of latex films with varying methacrylic acid content

Benjamin Voogt¹, Henk Huinink¹, Loes van de Kamp-Peeters¹,
Bart Erich^{1,2}, Jurgen Scheerder³, Paul Venema⁴, and Olaf Adan^{1,2}

¹Department of Applied Physics, Eindhoven University of
Technology, P.O. Box 513, Eindhoven, Netherlands

²TNO (The Netherlands Organization for Applied Scientific
Research), P.O. Box 49, Delft, Netherlands

³DSM Coating resins, P.O. Box 123, Waalwijk, Netherlands

⁴Laboratory of Physics and Physical Chemistry of Foods,
Wageningen University, Wageningen, The Netherlands

January 7, 2019

Abstract

The hydroplasticization of coatings of acrylic copolymers with different amounts of methacrylic acid (MAA) was investigated to clarify the role of carboxylic acid functionalities on the change in polymer mobility due to water uptake. The coating T_g as a function of water uptake was studied using dynamic mechanical analysis. The T_g 's decreased with increasing water content, confirming the plasticizing effect of water on the coatings. At relative humidities RH between 0 and 60% the coating T_g shows a sharper decrease than at higher RH , an effect that increases with increasing MAA content. This behavior is attributed to the presence

of dimers of carboxylic acid in the coatings, which is also observed with FTIR-ATR analyses. Due to water uptake, the dimers are disrupted and form "open" dimers where carboxylic acid groups remain in close proximity and are connected through water molecules. With ^1H NMR relaxometry, two T_2 relaxation times are found, representing two hydrogen pools with different mobilities. Both mobilities increase with increasing water content, indicating the presence of polymer domains with different hardness. Correlating the T_2 relaxation times with the coating T_g 's shows that at higher MAA content the proton mobility as a function of T_g of the soft domains increases with increasing MAA content. Since the polymer proton mobility, and hence the polymer mobility, is expected to scale with the polymer T_g , it is hypothesized that harder domains are present in the coatings, which are not visible in the Ostroff-Waugh decays due to the fast relaxation behavior of these protons.

1 Introduction

Paint is an abundantly used form of coating that provides substrates with a protective and, in most cases, aesthetic layer. Nowadays commercial paints are waterborne instead of solventborne as a result of stricter legislation, increasing environmental concern, and a consequent research focus on the development of aqueous paints in the past decades.

The main ingredient in waterborne paint is latex, submicrometer sized polymer particles dispersed in water, which during drying will form a close packing, deform, and ultimately bind a drying paint layer through interdiffusion of polymer chains [1]. This results in a mechanically and chemically robust coating. To promote the interdiffusion process, small amounts of organic co-solvent are added to the paint. This softens the latex particles by effectively lowering the glass transition temperature T_g of the polymer particles and therefore increase the mobility of the individual polymer chains. During drying this co-solvent will evaporate, which again increases the T_g and decreases the mobility of the polymers. The evaporation of the co-solvent unavoidably results in release of fumes

in the environment leading to societal concerns on environmental pollution and health issues.

A "holy grail" in paint research is the development of a latex, which will form a coating with similar physical, chemical, and mechanical properties as conventional paints without the need of any co-solvent. One possible way to achieve this goal is through hydroplasticization, where the polymer interdiffusion process is solely driven by the decrease of polymer T_g by water. Such hydroplasticization effect has been observed on multiple occasions, where small amounts of water were shown to promote deformation and interdiffusion of polymer particles [2, 3, 4, 5, 6]. One way to promote hydroplasticization is functionalization of the latex particles with hydrophilic groups. In that case, increased adsorption of water should lead to a decrease in polymer T_g and an increase in polymer mobility [7].

Soleimani and co-workers studied the diffusion of acrylic copolymers due to water uptake of coatings obtained after pre-drying the latex dispersions [6]. They indeed found that the mobility of the polymers increased upon hydroplasticization and that the composition of the polymer is crucial in this process. Although they compared two acrylic copolymers with similar T_g , but different hydrophilicity, a more systematic approach would be to vary the amount of one hydrophilic monomer and study the influence of this variation on the hydroplasticization process in the coatings.

In a study by Hong, the influence of concentration variations of hydrogen bonding monomers on polymer mobility has been presented [8]. It was shown that increased concentrations of this monomer increased the polymer T_g and decreased the polymer mobility. The polymer mobility, however, increased again after water uptake of the coatings. A relation between the water uptake and the polymer T_g and hence polymer T_g and polymer mobility, was not investigated. To our knowledge, studies on polymer mobility and T_g changes in coatings due to plasticization by water have not been done yet.

In the current work we present the results of a study on the hydroplasticization of polymers in coatings from acrylic latex dispersions with varying

amounts of methacrylic acid (MAA) and thus carboxylic acid functionalities. As a starting point it is imperative to understand how polymer T_g and polymer mobility change when water is adsorbed by the polymers. The polymer mobility is investigated using ^1H NMR relaxometry by monitoring the change of polymer proton mobility in acrylic coatings due to water uptake. The change of T_g of these coatings due to water uptake is studied using dynamic mechanical analysis (DMA). This ultimately allows us to investigate the relation between polymer T_g and mobility and the influence of polymer hydrophilicity on this relation. With this we aim to clarify the role of carboxylic acid functionalities on the hydroplasticization and the concomitant change in mobility of acrylic polymers.

2 Materials and methods

2.1 Latex synthesis

The following procedure describes the synthesis of the latex dispersion containing 2 wt% methacrylic acid (MAA) on total solid content. Table 1 lists the monomer amounts used for all latex dispersions. The solid weight fractions were determined gravimetrically.

A 2000 cm³ flask equipped with a thermometer, N₂ inlet and overhead stirrer was charged with water (799.1 g) and ammonium persulphate (0.35 g). In a funnel, an emulsified monomer feed was prepared by mixing demineralised water (305.97 g), sodium lauryl sulphate (4.62 g of 30 wt% solution in water), methyl methacrylate (MMA, 353.59 g), n-butyl acrylate (n-BA, 325.85 g) and methacrylic acid (MAA, 13.87 g). In another funnel, an initiator solution was charged by dissolving ammonium persulphate (3.12 g) in demineralised water (111.38 g). The reactor was heated to 83 °C and 5 wt% of the emulsified monomer feed was added to the reactor and the reaction temperature was allowed to increase to 85 °C. At 83-87 °C, the remainder of the monomer mixture was fed to the reactor in 100 minutes. At the end of the monomer feed deminer-

Table 1: Monomer amounts (wt% on total solids) of methacrylic acid (MAA), methyl methacrylate (MMA), and n-butyl acrylate (n-BA) and the total solid contents (wt%) of the latex dispersions used for this study.

MAA	MMA	n-BA	latex solid content
2.0	51.0	47.0	33.8
5.0	47.0	48.0	34.1
10.0	40.4	49.6	33.6
15.0	33.7	51.3	30.5
20.0	27.0	53.0	21.7

alised water (28.3 g) was used to rinse the funnel holding the monomer mixture. The reaction was kept at 85 °C for 30 minutes. Next, the batch was cooled to room temperature and Proxel Ultra 10 (6.9 g of a 10 wt% solution) was added to prevent bacterial growth, followed by demineralised water (45.3 g). Finally, the batch was filtered through a filter cloth to remove any coagulum formed during the reaction. To adjust the pH a dilute solution of ammonia (5 wt% in water) was added under mild stirring.

Since no chain transfer agent was used for the synthesis, molecular weights $\gg 100,000$ Da of the polymers **and monomer conversion degrees >99.95% are obtained** [9]. Hence, polymers with high amounts of MAA will not dissolve at $\text{pH} > 7$, which is confirmed by particle size measurements showing similar sizes for all dispersions with narrow distributions. **Moreover, free monomer present in the coatings will have a negligible effect on the plasticization and hydroplasticization of the coatings.** The average particle diameter (Z_{av}) and polydispersity index (\mathfrak{D}) were determined by dynamic light scattering (Malvern Zetasizer Nano ZS) at 25 °C. Results of the analyses are listed in table 2.

Table 2: Physical characteristics of the latices. Z_{av} is the average particle diameter and \mathfrak{D} the polydispersity index of the size distribution of the latex.

latex (% MAA)	Z_{av} (nm)	\mathfrak{D}
2	345	0.04
5	323	0.06
10	308	0.05
15	301	0.07
20	293	0.03

2.2 GARField ^1H NMR

The principles of GARField ^1H NMR have first been described by Glover *et al.*[10] The magnetic field strength of the equipment used for this study was 1.5 T and the static gradient was 35.0 ± 0.2 T/m. An Ostroff-Waugh [11] pulse sequence ($90_x^\circ-\tau-[90_y^\circ-\tau\text{-echo}-\tau]_n$) was used to obtain T_2 relaxation times of polymer protons. The echo time $t_e=2\tau$ used for this study is $40 \mu\text{s}$ with an acquisition time t_{ac} of $35 \mu\text{s}$, resulting in a spatial resolution of $14 \mu\text{m}$. The long delay l_d was set at 0.5 s and the number of echoes n at 128. To reduce the signal-to-noise ratio, an average of 1024 measurements was used. The results were normalized with a reference signal, obtained by a measurement of an aqueous 0.025 M CuSO_4 solution with $t_e = 40\mu\text{s}$, $t_{ac} = 35\mu\text{s}$, $l_d = 0.3$ s, $n = 2048$ and 4096 averages.

The signal decays of the coatings at the various RH obtained with the Ostroff-Waugh pulse sequence can be fitted with an exponential decay function,

$$S_n(x) = P_n(x) \sum_{k=1}^N A_k(x) \exp\left(\frac{-nt_e}{T_{2,k}(x)}\right) + S_0 \quad (1)$$

where $S_n(x)$ [a.u.] is the total signal at time $t=nt_e$ [s], $T_{2,k}(x)$ [s] is the transversal relaxation time of the k th proton pool of the sample with amplitude $A_k(x)$ [a.u.], and S_0 [a.u.] is the signal noise level. The weighing factor $P_n(x)$, necessary to correct for the coil profile and echo modulations introduced by the Ostroff-Waugh sequence, is obtained using an aqueous 0.025 M CuSO_4 solution. We refer to [12] for more details. Equation 1 can be re-written as

$$I_n(x) = \sum_{k=1}^N \frac{A_k(x)}{A_{ref}(x)} \exp\left(\frac{-nt_e}{T_{2,k}(x)}\right) = \sum_{k=1}^N \rho_k(x) \exp\left(\frac{-nt_e}{T_{2,k}(x)}\right) \quad (2)$$

where $I_n(x)$ is the relative signal intensity and $\rho_k(x)$ the relative proton density of the k th proton pool with respect to water. $A_{ref}(x)$ is the signal amplitude obtained with the reference measurement of the CuSO_4 solution.

In order to obtain Ostroff-Waugh signal decays of the different coatings with different water saturation levels, the NMR set-up is equipped with a temperature and humidity controlled chamber in which the sample holder with the coating sample is placed directly onto the RF coil. The temperature in the chamber is controlled by a temperature-controlled water flow through the walls of the chamber. The chamber RH is generated by an air flow into the chamber with a partial water vapor pressure, obtained by premixing dry and water saturated air in a ratio depending on the desired RH .

The sample holder is a 140 μm thick cover glass covered with a microscope object glass having a circular hole of 10 mm diameter. Coating samples were prepared for measurement in three steps. First, 60 μL of latex dispersion was placed in the sample holder using a 100 μL volumetric pipette in the sample holder. The sample holder was then placed in a dessicator containing a saturated aqueous KCl solution, which in equilibrium provides a stable relative humidity (RH) of 85% at room temperature. Second, after 48 hours the sample holder was placed in a closed box containing anhydrous CaCl_2 at room temperature, providing a RH close to 0%, to remove residual water from the coating. Third,

to saturate coating samples at a desired RH , mixtures of water and anhydrous glycerol were made according to [13], which give an equilibrium RH depending on their mixing ratio. The NMR sample holder with sample was placed in a closed box containing a water-glycerol mixture. After 48 hours the sample holder was weighed to monitor the weight increase due to water uptake and a ^1H NMR measurement was done at $23\text{ }^\circ\text{C}$ with the climate chamber set at the same RH used for pre-conditioning of the sample with the water-glycerol mixtures. The water fraction θ [wt%] was calculated using

$$\theta = \frac{m_{tot} - m_0}{m_0} \times 100\%, \quad (3)$$

with m_{tot} [g] the total mass of the coating sample after each RH equilibration step and m_0 [g] the mass of the sample after drying with CaCl_2 . Subsequently, a new ^1H NMR measurement was performed. This was repeated at RH ranging from 10 to 90% in 10% steps.

2.3 Dynamic mechanical analysis

Dynamic mechanical analysis (TA Instruments DMA Q800) equipped with a humidity control chamber was done at fixed humidities to determine coating T_g as a function of RH . Measurements were done at an oscillation frequency of 1 Hz and with an amplitude of $10\text{ }\mu\text{m}$. The heating rate was set at $1\text{ }^\circ\text{C}/\text{min}$. Samples were prepared by drawing a latex layer on a polypropylene plate, cleaned prior with demineralized water and isopropanol, using a $300\text{ }\mu\text{m}$ drawdown bar and allowing it to dry for at least 48 hours under ambient conditions. Samples were cut with a constant width of 5.3 mm for all samples. The sample thickness was variable and was determined individually for each sample prior to measurement. Samples were equilibrated in the humidity control chamber at $25\text{ }^\circ\text{C}$ at the RH used for the measurement until constant shear storage (G') and loss (G'') moduli were observed. By convention, the T_g of the coating is taken at the maximum of the loss tangent $\tan(\delta)$

$$\tan(\delta) = \frac{G''}{G'}. \quad (4)$$

2.4 FTIR-ATR

Surface properties of the coatings were probed using FTIR (Shimadzu FTIR 8400S) equipped with a horizontal ATR (Attenuated Total Reflection) crystal to investigate changes in the molecular structure due to water uptake. The penetration depth of light ranges from approximately $0.5 \mu\text{m}$ at wavenumber 4000 cm^{-1} to $5 \mu\text{m}$ at 400 cm^{-1} . Hence, FTIR-ATR mostly provides information on the surface composition of the coatings, but it can still be used for qualitative assessment on the role of carboxylic acid groups on the water uptake. Before analysis, the crystal surface was thoroughly cleaned with a tissue soaked in isopropanol and left to dry. The coating material was applied on the surface of the crystal and the spectrum was collected by co-adding 32 scans at a resolution of 4.0 cm^{-1} and automatic gain. The coating preparation procedure was similar to the DMA preparation procedure described in section 2.3. Pieces of the coatings were placed in desiccators containing saturated salt solutions, which give equilibrium RH as described in [14]. Dry coating pieces were prepared in a dessicator containing dry silica gel granules. After at least 48 hours of equilibration, spectra were measured.

Underlying bands in FTIR spectra in the $1580 - 1800 \text{ cm}^{-1}$ vibration range were distinguished using a Gaussian peak function to fit the data

$$\text{Abs}_i(x) = \frac{A_i}{w_i \sqrt{\pi/2}} e^{-2\left(\frac{x_i - x_{c,i}}{w_i}\right)^2}, \quad (5)$$

with $\text{Abs}_i(x)$ the absorbance of band i at wavenumber x_i [cm^{-1}], w [cm^{-1}] the width at half of the maximum of the band, $x_{c,i}$ [cm^{-1}] the peak center, and A_i the band area.

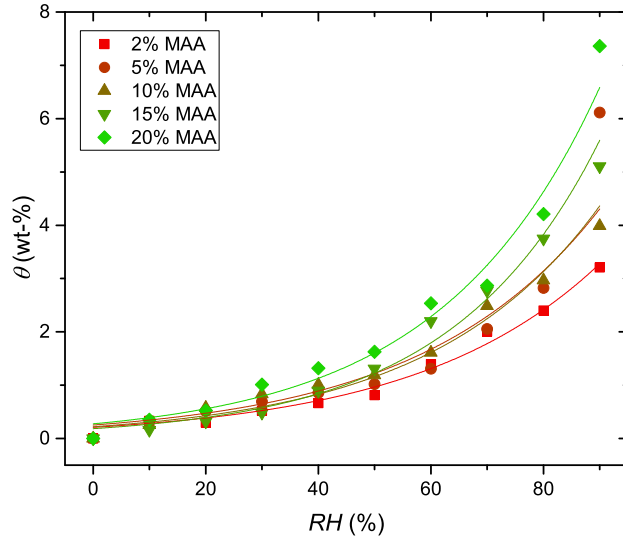


Figure 1: The absorption isotherms of coatings for different values of the relative humidity RH at 23 °C. Lines drawn to guide the eye show the trends of increased water uptake with increasing RH and MAA content.

3 Results

3.1 Water absorption isotherms

Carboxylic acid groups can bind relatively high amounts of water, and are therefore expected to have a significant impact on the coating T_g . [7]. Therefore, the water content θ of one coating from each latex dispersion was determined after each RH step. The water uptake of the coatings was monitored by weighing the 1H NMR samples after each RH step and θ was calculated with Eq. 3. Figure 1 shows the results.

The dependency of coating water uptake on MAA content is obviously underlined, as is stressed by the trend lines drawn in Figure 1. With increasing RH , θ increases for each coating. With an increasing number of carboxylic acid groups, the water content also increases, being in line with expectations

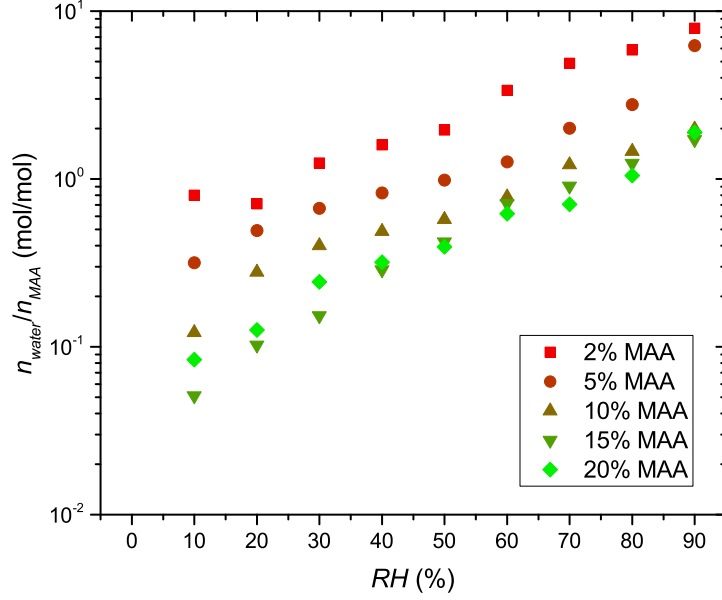


Figure 2: Ratio of the amount of water molecules n_{water} and acid functionalities n_{MAA} of the various coatings as a function of relative humidity RH .

that acid groups are binding sites for water due to their hydrogen bonding capability.[7] Another observation, however, is that θ at any RH does not scale with the acid group concentration. To provide better insight, Figure 2 shows the ratio of water molecules n_{water} [mol] and acid groups n_{MAA} [mol] as a function of RH for all coatings.

As can be seen, n_{water}/n_{MAA} is not equal for all the coatings at the individual RH 's. With increasing MAA content, less water is absorbed per carboxylic acid group. From 10% MAA and higher, in particular at 60% RH and higher, the amount of water per carboxylic acid group reaches an equilibrium value. This suggests that water absorption by the coating is hindered. A plausible explanation could be the confinement of the coating samples. Sample volumes increase by water sorption, and the concomittant strain increase prevents the

samples from reaching their water saturation levels [15, 16].

3.2 FTIR analysis

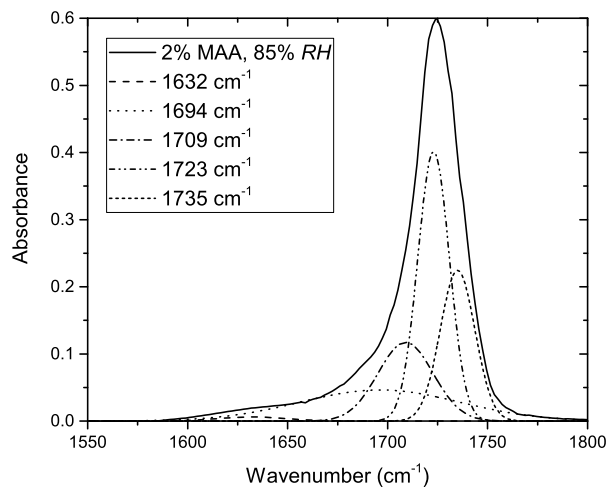
Despite the fact that carboxylic acid groups in the coatings are the main contributors to hydroplasticization of the polymers [7], the water uptake effects on molecular interactions in the coatings are not fully understood. FTIR-ATR measurements were done to elucidate this. In the FTIR spectra, two vibration ranges are of interest. First, in the range between 1550 and 1800 cm^{-1} , C=O stretch vibrations of the carboxylic acids and esters are found, of which the former are expected to be affected mostly by water uptake. Second, in the range between 2400 and 4000 cm^{-1} O-H stretch vibrations are found, of which the intensity should increase with water uptake by the coatings. In figure 3 the FTIR spectrum vibration range 1550-1800 cm^{-1} of the 2% and 20% MAA coatings at 85% *RH* are shown.

Figure 3 clearly shows differences in the shape of the spectrum depending on the carboxylic acid content of the coatings. To elucidate these differences, it is necessary to identify underlying bands of C=O stretch vibrations of different origins. Using Gaussian peak fits as described in section 3.2, five bands are found. These bands are listed in Table 3 with the attributed vibration types.

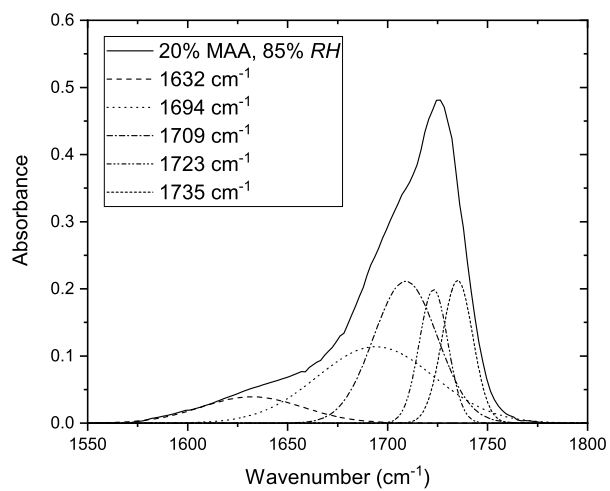
Due to the incorporation of three different acrylic monomers on the polymers, three different carbonyl groups are present. Two carbonyl groups are part of the ester functionalities of MMA and BA and one carbonyl group is part of the carboxylic acid functionality of MAA.

The areas of the bands at 1723 and 1735 cm^{-1} , shown in figure 3 are hardly affected by water uptake, and are therefore attributed to the ester C=O moieties of MMA and BA, respectively. Fig. 4a shows that the band area ratios of the coatings at 1723 and 1735 cm^{-1} (A_{1723}/A_{1735}) are rather constant. Moreover, they scale linearly with the molar ratio of MMA and BA, as shown in Fig. 4b for the coatings at 0% *RH*, supporting this attribution.

Carboxylic acid groups can show up in an FTIR spectrum in different forms



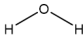
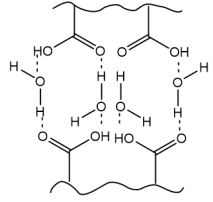
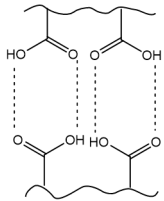
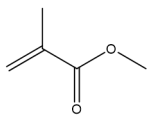
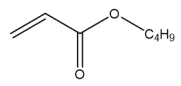
(a)

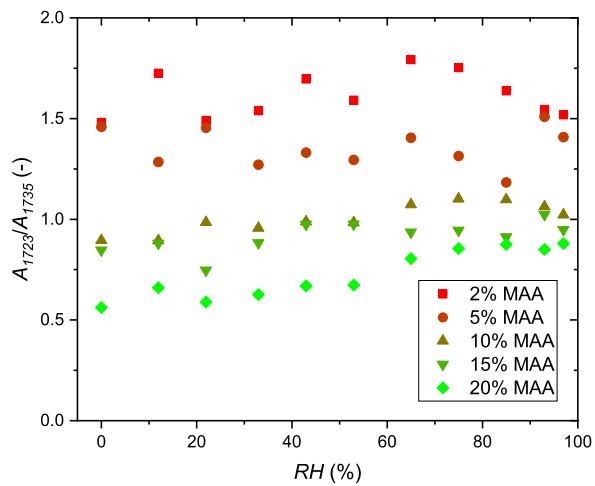


(b)

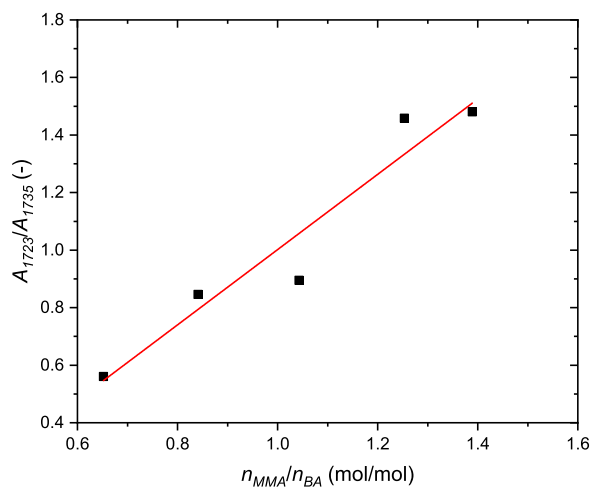
Figure 3: FTIR spectrum range of 1550 - 1800 cm^{-1} of (a) the 2% MAA coating at 85% *RH* and (b) the 20% MAA coating at 85% *RH*. Gaussian fits are applied to distinguish underlying bands.

Table 3: Underlying bands found in the FTIR vibration range $1550 - 1800 \text{ cm}^{-1}$ with their respective attributions. The positions of the water O-H bending vibration and the carboxylic acid C=O stretch vibrations are based on those found in [17]

Wavenumber cm^{-1}	vibration type	molecular conformation
1632	O-H bending vibration (water)	
1694	C=O stretch vibration (open dimer)	
1709	C=O stretch vibration (dimer)	
1723	C=O stretch vibration (MMA ester)	
1735	C=O stretch vibration (BA ester)	



(a)



(b)

Figure 4: (a) Area ratios of the bands at 1723 (A_{1723}) and 1735 (A_{1735}) cm^{-1} of the various coatings attributed to C=O stretch vibrations of MMA and BA, respectively. (b) Band area ratios A_{1723}/A_{1735} at 0% RH versus the molar ratio of MMA and BA n_{MMA}/n_{BA} .

due to the possibility of dimerization through hydrogen bonding [18, 17, 19]. Hence, both dimers and free carboxylic acid groups, not bound to other carboxylic acid groups, could be expected. It is known, however, that free carboxylic acid groups are hardly visible in the spectrum suggesting that the dimerized state is the preferential conformation [20]. In the presence of water, dimers are broken and form so-called "open dimers", which appear as a broad band due to the variety of possible spatial conformations [18, 17]. The dimers and open dimers are found at 1709 and 1694 cm^{-1} , respectively. Direct comparison of the band areas of the different coatings is, however, not possible. Peak intensities depend on the penetration depth of the light into the coating samples, which in turn depend on the coating refractive index n_c [21]. Therefore, variations in coating composition due to MAA or water concentration can impact peak intensities. Band area ratios, however, can still provide information on the conversion of dimers to open dimers. As shown in Fig. 5, upon water absorption, the area ratio of these bands A_{1694}/A_{1709} increases, indicating dissociation of the cyclic dimers into open dimers. The presence of open dimers at 0% RH could indicate that residual water is still present in the coating.

An additional broad band is observed at 1632 cm^{-1} , which is known to originate from O-H bending vibrations of free water in the coating [17, 19, 18]. The O-H stretching vibrations of water at approximately 3400 cm^{-1} , however, give stronger absorbance and therefore provide more accurate information on the water absorption. Hence, these bands are used to assess water sorption by the coatings.

Fig. 6a shows the FTIR spectrum vibration range between 2400 and 4000 cm^{-1} of the 2% MAA coating. In this range, C-H stretching vibrations of alkyl groups at 2874 and 2955 cm^{-1} and O-H stretching vibrations of the carboxylic acid groups at approximately 3200 cm^{-1} are visible, which are not significantly affected by the water uptake of the coatings. By integration of the spectrum areas between 2400 and 4000 cm^{-1} and normalization with the C=O stretching band of the BA ester at 2935 cm^{-1} , information on the water uptake is obtained, as shown in figure 6b. Figure 6 shows the areas of these peaks A_{OH}

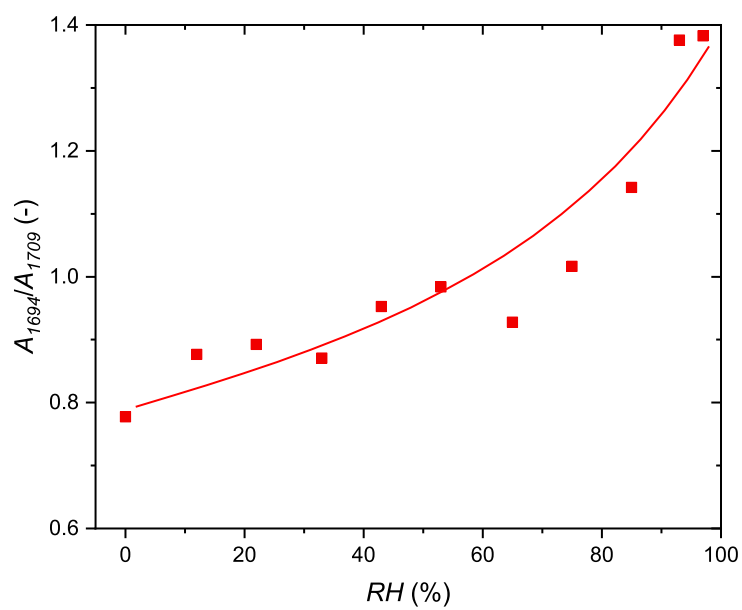


Figure 5: Ratio of the FTIR band areas at 1694 (A_{1694}) and 1709 (A_{1709}) cm^{-1} of the 2% coating, representing open dimers and cyclic dimers of carboxylic acid respectively. A trendline is drawn to guide the eye. Data for the 5, 10, 15 and 20% coatings are not shown for the sake of clarity.

normalized with the BA band at 1735 cm^{-1} . For the 20% MAA coating, a gradual increase in the amount of free water occurs. For the other coatings, however, the amount of free water is about constant up to approximately 60% RH . At higher humidities the amount of free water in these coatings increases more significantly.

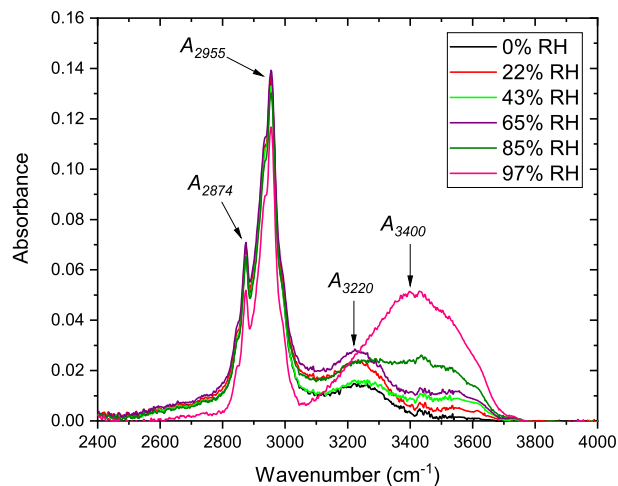
3.3 Coating proton mobility

Polymer mobility in a coating is expected to change when water is absorbed. Inter- and intramolecular bonds are broken leading to a higher degree of freedom for the polymer chains. The polymer mobility is directly related to proton mobility, which can be quantified using NMR relaxometry. In figure 7 an example of Ostroff-Waugh signal decays at different RH are shown for a coating containing 10% MAA. The T_2 relaxation times increase with increasing water absorption by the coatings.

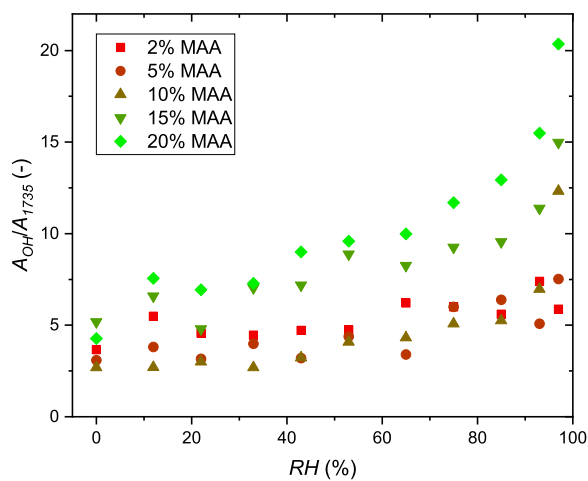
After equilibration at higher RH , the T_2 relaxations of the coating increase due to water uptake. The relaxation times are obtained with a bi-exponential fit of the Ostroff-Waugh signal decay using equation (2) with $k = 2$, meaning that two pools of protons with different mobilities are found. In figures 8a and b relaxation times $T_{2,1}$ and $T_{2,2}$ for all coatings are shown as a function of θ . Figures 8c and d show their respective proton densities ρ_1 and ρ_2 .

Both T_2 relaxations increase with increased coating water content. The proton mobility appears to be directly related to the water content of the coatings. The MAA content, however, does not obviously influence T_2 : It is the higher coating water content with higher MAA content that determines the increase in proton mobility.

Proton densities ρ_1 and ρ_2 as a function of θ show a rather scattered pattern, with no distinct effect of water uptake. This can be explained by the relatively low contribution of water protons to the total signal intensity I , as is shown in figure 9, which is within the noise levels of the measurements. Consequently, polymer protons with a different degree of mobility apparently dominate the



(a)



(b)

Figure 6: (a) FTIR spectrum of the 2% MAA coating between 2400 and 4000 cm^{-1} , with at 2874 and 2955 cm^{-1} alkyl C-H stretching vibrations and at 3220 and 3400 cm^{-1} O-H stretching vibrations of carboxylic acid groups and water, respectively. (b) Integrated area between 2400 and 4000 cm^{-1} (A_{OH}) normalized with the BA band area at 1735 cm^{-1} as a function of RH for varying MAA content.

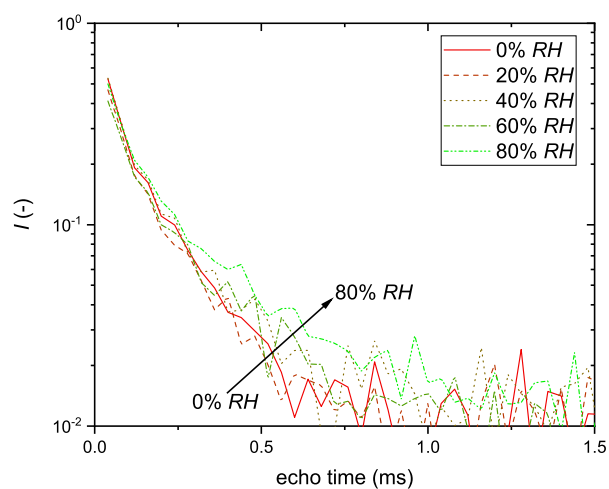


Figure 7: Ostroff-Waugh signal decays of a coating with 10% MAA after equilibration at different RH . The signal intensity I decays with each echo due to transversal relaxation of the hydrogens. The relaxation time T_2 is linked to the hydrogen mobility. An increased relaxation time, and hence a slower signal decay, indicates an increased hydrogen mobility. This is the case for the coating hydrogens when water is absorbed.

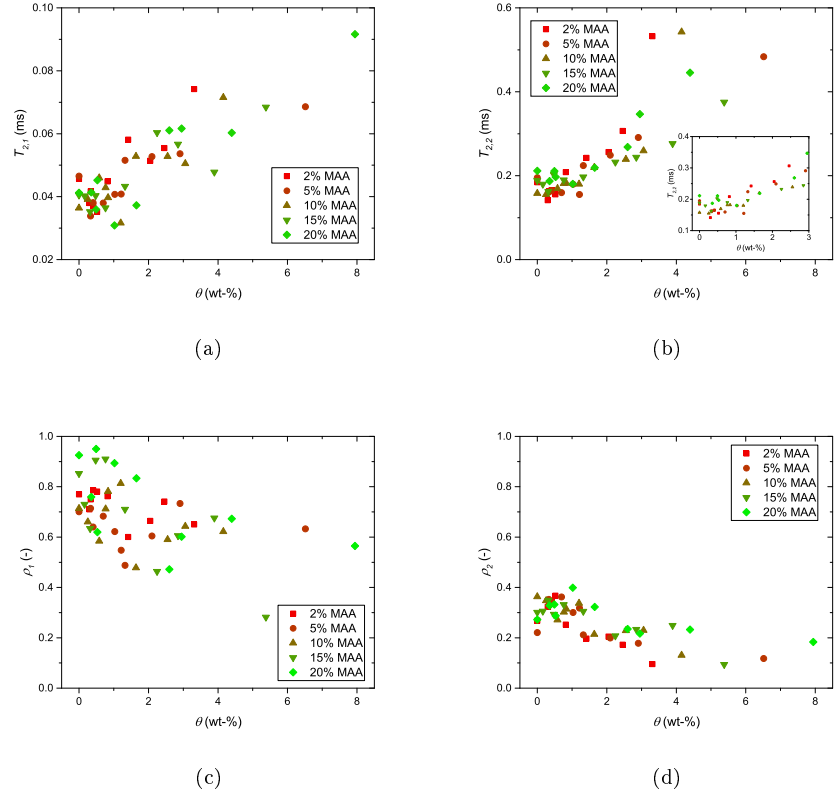


Figure 8: (a) The short ($T_{2,1}$) and (b) long ($T_{2,2}$) T_2 relaxations of the various coatings obtained by a double exponential fit of the Ostroff-Waugh signal decays using equation 2 and their respective relative proton densities (c) ρ_1 and (d) ρ_2 . The insert in figure (b) magnifies the $T_{2,2}$ relaxations at lower θ to clarify that no significant differences are observed for different MAA contents. Note that the data in figures (a) and (c) are more scattered compared to those in figures (b) and (d) due to the limited amount of data points available in the Ostroff-Waugh decays.

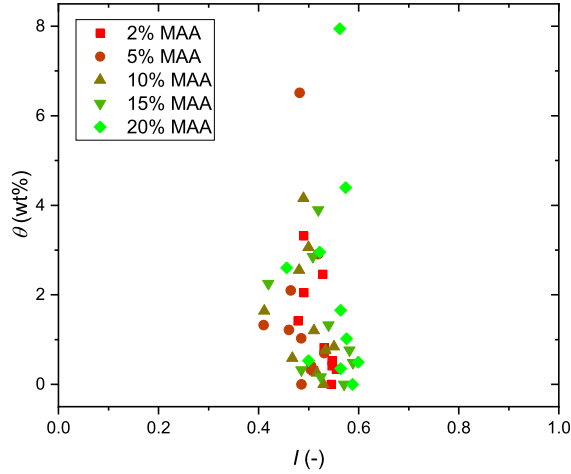


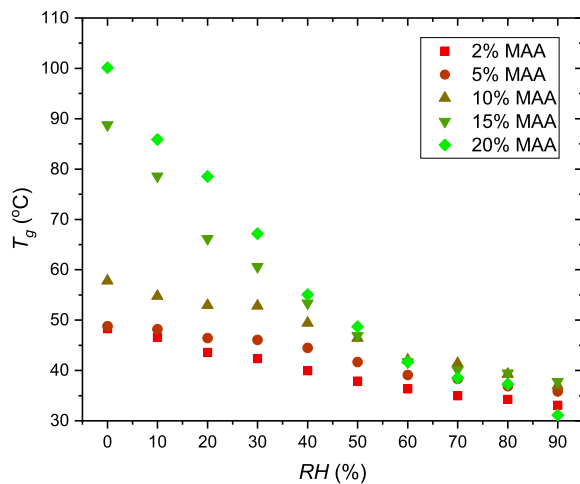
Figure 9: θ versus the signal intensity I of the first echo of the Ostroff-Waugh signal decays of all coatings.

$T_{2,1}$ and $T_{2,2}$ relaxations.

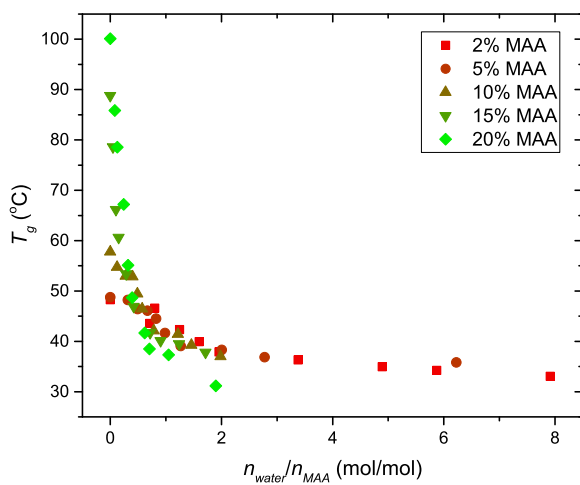
3.4 Coating T_g

The coating T_g decreases when water is absorbed. Water disrupts molecular interactions leading to softening of the coating. DMA was used to quantify the effective T_g of the coatings as a function of RH . In figure 10a results of the measurements are shown as a function of θ .

As expected, the T_g of the coatings decreases with increasing RH . Obviously, the T_g of the coatings under dry conditions increases with increasing MAA content. This is expected due to the positive contribution of MAA to the polymer T_g [7]. With increasing RH , the coating T_g 's converge to approximately 35-40 °C. Furthermore, obviously there is a more pronounced effect for MAA coatings above 10% at lower RH . It is hypothesized that **the dimerization of carboxylic acid groups has a much more pronounced effect on the coating T_g at lower RH at high MAA content, which contributes to an increased coating T_g .**



(a)



(b)

Figure 10: (a) Glass transition temperatures T_g of the various coatings obtained by dynamic mechanical analysis as a function of RH . (b) T_g 's of the various coatings as a function of the molar water and MAA ratio n_{water}/n_{MAA} .

By plotting the T_g as a function of the water and MAA molar ratio n_{water}/n_{MAA} , as is shown in figure 10b, the role of MAA on the T_g decrease due to water uptake can be studied. The result shows that the data are almost superimposing, indicating the dominant role of the carboxylic acid groups in the hydroplasticization process.

3.5 Discussion

The water uptake studies in section 3.1 show that an increasing MAA content also increases the total amount of water that is absorbed by the coating at a given RH . When considering the relative amount of water, i.e. the amount of water bound per MAA monomer, a steady decrease is observed down to an amount that obviously not differs significantly for 10 wt% MAA and higher. This might reasonably indicate a limiting factor in the water uptake of the coatings. For example, the diffusion of water and the water saturation levels in a coating are stress dependent, meaning that strain increase due to confinement of the coating can inhibit the water uptake [15, 16]. This would imply that coatings with higher MAA contents can not reach their water saturation levels, resulting in lower molar water and MAA ratios.

FTIR-ATR measurements of the coatings show that carboxylic acid groups are predominantly present as cyclic dimers in the coatings. This may explain the T_g values found with DMA as is shown in figure 10. With an increasing amount of MAA in the coating, the amount of carboxylic acid dimers also increases, which in turn increases the coating T_g . Apparently, this effect becomes more dominant at carboxylic acid contents of 10% and higher. Upon water uptake, the carboxylic acid dimers are disrupted. Although it might be expected that this would result in free carboxylic acid groups, it is known that mostly "open" dimers are formed [18, 17, 19]. Carboxylic acid groups remain in close proximity and are connected by water molecules.

This behavior provides a plausible explanation for the proton mobilities found, as shown in figure 8. Due to continuing interaction of carboxylic acid

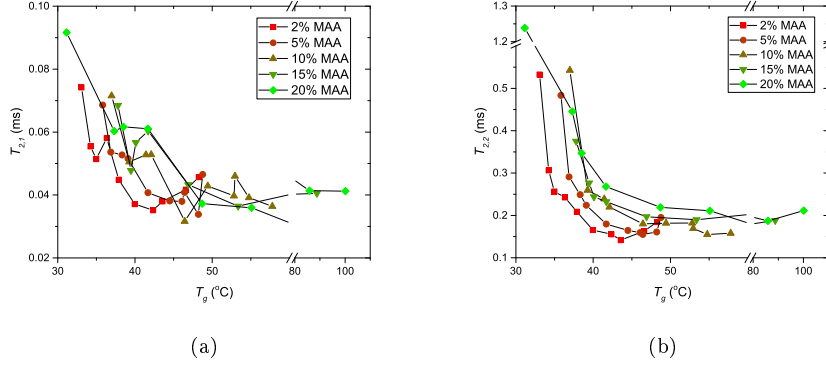


Figure 11: The polymer proton mobilities represented by $T_{2,1}$ (up) and $T_{2,2}$ (down) relaxation times as a function of polymer T_g .

groups in the open dimers, polymer mobilities, and hence proton mobilities, do not increase a lot after disruption of the cyclic dimers. The T_2 relaxation times indeed show an increase with increasing water content, but still remain rather short. Moreover, there are no significant differences between the relaxation time of the different coatings, which are to be expected based on the large differences between the T_g 's of the various coatings at $\theta < 3$ wt% (see figure 10a). Hence, increasing the carboxylic acid content of the coatings does not significantly influence the polymer mobility of the coatings after water uptake at similar θ . It merely provides the coatings with additional hydrogen bonding sites to increase θ , and hence the polymer mobilities, at similar RH .

Correlating both T_g and T_2 can provide more insight into the change in polymer mobility due to a decrease in T_g . In figure 11, the T_2 dependence on T_g of different coatings is shown for all coatings.

In general, a clear relation between T_2 relaxation times, and therefore polymer mobilities, and coating T_g is found. Both shorter $T_{2,1}$ and longer $T_{2,2}$ relaxations show a decrease in polymer proton mobility with an increase of the coating T_g , and thus the glassy character, for all coatings. Unfortunately, the $T_{2,1}$ relaxation data are scattered as a result of the limited amount of data

points available for fitting of the Ostroff-Waugh decay. Hence, it is not possible to observe potential differences between the various coatings.

The $T_{2,2}$ relaxation times as a function of coating T_g show clearer results. First, for all coatings a gradual decrease in proton mobility is seen between T_g 's of approximately 35 and 45 °C. At an ambient temperature of 23 °C, a transition from a rubber-like to a glassy state of polymer segments is expected in this range. At higher T_g 's the proton mobilities do not decrease significantly anymore, an indication that the mobility of the polymers segments has reached a minimum.

At T_g values between 35 and 45 °C, proton mobilities at any given T_g appear to increase with increasing MAA content. Since both polymer T_g and T_2 are measures of the mobility of the polymer, the curves in figure 11a and b should superimpose. At least for $T_{2,2}$, this is clearly not the case. An explanation for this is the presence of hydrogen pools in the coating with relaxation times $T_2 < t_e$. In other words, if $T_2 < 40\mu\text{s}$, this would not appear in the Ostroff-Waugh signal decay. The size of such hydrogen pools should thus increase with increasing MAA content, as this would decrease the average T_2 .

4 Conclusion

Plasticization of a polymer by water, also known as hydroplasticization, brings about a decrease in the effective glass transition temperature T_g and therefore increases the polymer mobility. The hydroplasticization process in acrylic coatings with different amounts of acid groups in the form of methacrylic acid (MAA) has been studied as a function of water content.

The water content θ of the coatings increased with an increase of the relative humidity (RH). This is promoted by the presence of MAA in the coating due to the hydrogen bonding capability of carboxylic acid groups. Concomitantly, the T_g 's of the coatings decrease and the T_2 relaxation times, measured with ^1H NMR relaxometry, increase. Hence, polymer mobilities in the coatings increase due to the hydroplasticization effect during water uptake.

The coating T_g decreases with water uptake as a result of the hydroplasticization of the polymers. In dry conditions, the T_g of the coatings increases with an increase of the MAA content. This is explained by the presence of dimers of carboxylic acid groups in the coatings, of which the concentration increases with increasing MAA content. These dimers increase the coating T_g .

Correlating the T_2 relaxation times of the softer polymer domains with the coating T_g shows higher mobilities as a function of T_g with increasing MAA content. The presence of hydrogen pools with even lower mobilities, which can not be measured due to their fast relaxation, could provide a plausible explanation for this observation.

Acknowledgements

This work is part of the research programme True Solvent Free (TSoF) - Towards the next generation of waterborne coatings with project number 13157, which is (partly) financed by the Netherlands Organisation for Scientific Research (NWO). Additional funding is provided by DSM Coating Resins, AkzoNobel N.V., Teknos Drywood, and Océ-Technologies B.V.. The authors would like to thank Joseph Keddie (University of Surrey) for his valuable feedback.

References

- [1] Joseph L Keddie and Alexander F Routh. *Fundamentals of Latex Film Formation*. Springer, Dordrecht, The Netherlands, 1 edition, 2010.
- [2] P. R. Sperry, B. S. Snyder, M. L. O’Dowd, and P. M. Lesko. Role of Water in Particle Deformation and Compaction in Latex Film Formation. *Langmuir*, 10(8):2619–2628, 1994.
- [3] F. Lin and D. J. Meier. A Study of Latex Film Formation by Atomic Force Microscopy. 1. A Comparison of Wet and Dry Conditions. *Langmuir*, 11(7):2726–2733, 1995.
- [4] F. Lin and D. J. Meier. A Study of Latex Film Formation by Atomic Force Microscopy. 2. Film Formation vs Rheological Properties: Theory and Experiment. *Langmuir*, 12(11):2774–2780, 1996.
- [5] Bo Jiang, John Tsavalas, and Donald Sundberg. Measuring the glass transition of latex-based polymers in the hydroplasticized state via differential scanning calorimetry. *Langmuir*, 26(12):9408–9415, 2010.
- [6] Mohsen Soleimani, Jeffrey C. Haley, Willie Lau, and Mitchell A. Winnik. Effect of Hydroplasticization on Polymer Diffusion in Poly(butyl acrylate-co-methyl methacrylate) and Poly(2-ethylhexyl acrylate-co-tert-butyl methacrylate) Latex Films. *Macromolecules*, 43(2):975–985, 2010.
- [7] John G. Tsavalas and Donald C. Sundberg. Hydroplasticization of polymers: Model predictions and application to emulsion polymers. *Langmuir*, 26(10):6960–6966, may 2010.
- [8] Seungmin Hong, Mohsen Soleimani, Yuanqin Liu, and Mitchell A. Winnik. Influence of a hydrogen-bonding co-monomer on polymer diffusion in poly(butyl acrylate-co-methyl methacrylate) latex films. *Polymer*, 51(14):3006–3013, 2010.

- [9] Jurgen Scheerder, Remy Dollekens, and Harm Langermans. The colloidal properties of alkaline-soluble waterborne polymers. *Journal of Applied Polymer Science*, 135(17):1–11, 2018.
- [10] P M Glover, P S Aptaker, J R Bowler, E Ciampi, and P J McDonald. A novel high-gradient permanent magnet for the profiling of planar films and coatings. *Journal of magnetic resonance (San Diego, Calif. : 1997)*, 139(1):90–7, jul 1999.
- [11] E. D. Ostroff and J. S. Waugh. Multiple spin echos and spin locking in solids. *Physical Review Letters*, 16(24):1097–1099, 1966.
- [12] Viktor Baukh, Hendrik P Huinink, Olaf C G Adan, Sebastiaan J F Erich, and Leendert G J Van Der Ven. Water-polymer interaction during water uptake. *Macromolecules*, 44(12):4863–4871, 2011.
- [13] Charles F Forney and David G Brandl. Control of Humidity in Small Controlled-environment Chambers using Glycerol-Water Solutions. *Hort Technology*, 2(1):52–54, 1992.
- [14] Lewis Greenspan. Humidity Fixed Points of Binary Saturated Aqueous Solutions. *Journal of Research of the National Bureau of Standards -A. Physics and Chemistry*, 81(1), 1977.
- [15] Y. Weitsman. Stress assisted diffusion in elastic and viscoelastic materials. *Journal of the Mechanics and Physics of Solids*, 35(1):73–94, 1987.
- [16] Chien H. Wu. The role of Eshelby stress in composition-generated and stress-assisted diffusion. *Journal of the Mechanics and Physics of Solids*, 49(8):1771–1794, 2001.
- [17] M. Hoerter, A. Oprea, N. Bârsan, and U. Weimar. Chemical interaction of gaseous ammonia and water vapour with polyacrylic acid layers. *Sensors and Actuators, B: Chemical*, 134(2):743–749, 2008.

- [18] Jian Dong, Yukihiro Ozaki, and Kenichi Nakashima. Infrared, Raman, and near-infrared spectroscopic evidence for the coexistence of various hydrogen-bond forms in poly(acrylic acid). *Macromolecules*, 30(4):1111–1117, 1997.
- [19] M. Todica, R. Stefan, C. V. Pop, and L. Olar. IR and Raman investigation of some poly(acrylic) acid gels in aqueous and neutralized state. *Acta Physica Polonica A*, 128(1):128–135, 2015.
- [20] Kevin W. Evanson and Marek W. Urban. Surface and interfacial FTIR spectroscopic studies of latexes. I. Surfactant - copolymer interactions. *Journal of Applied Polymer Science*, 42(8):2287–2296, 1991.
- [21] N. J. Harrick. Electric Field Strengths at Totally Reflecting Interfaces. *Journal of the Optical Society of America*, 55(7):851, 1965.